Molecular Cell, **Volume 83**

Supplemental Information

Histone H3 Lysine 27 Crotonylation Mediates Gene Transcriptional Repression in Chromatin

Nan Liu, Tsuyoshi Konuma, Rajal Sharma, Deyu Wang, Nan Zhao, Lingling Cao, Ying Ju, Di Liu, Shuai Wang, Almudena Bosch, Yifei Sun, Siwei Zhang, Donglei Ji, Satoru Nagatoishi, Noa Suzuki, Masaki Kikuchi, Masatoshi Wakamori, Chengcheng Zhao, Chunyan Ren, Thomas Jiachi Zhou, Yaoyao Xu, Jamel Meslamani, Shibo Fu, Takashi Umehara, Kouhei Tsumoto, Satoko Akashi, Lei Zeng, Robert G. Roeder, Martin J. Walsh, Qiang Zhang, & Ming-Ming Zhou

Figure S1, related to Figure 1

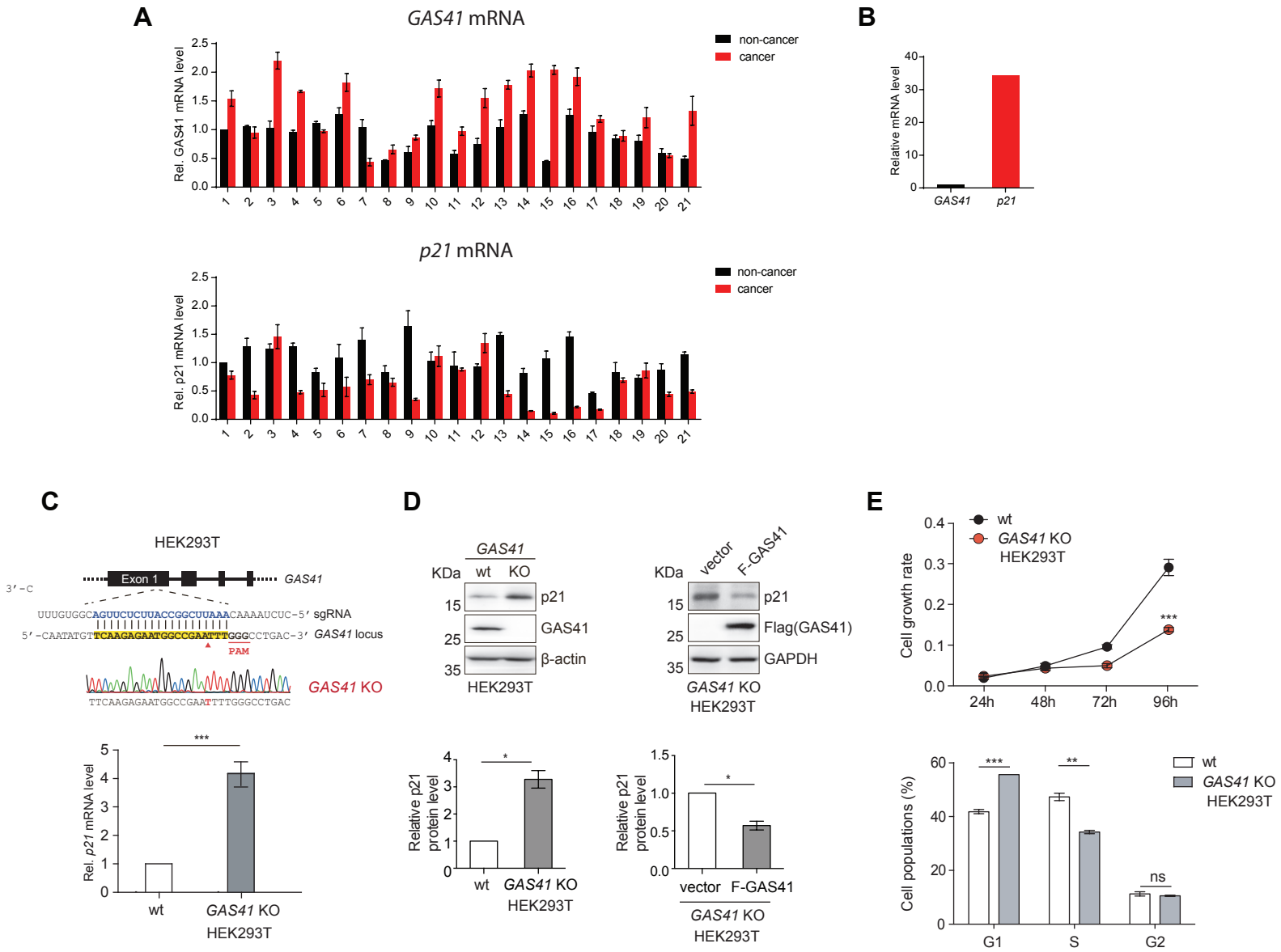

Figure S1. GAS41 represses *p21* expression in HEK293T cells, related to Figure 1.
(A) Relative mRNA expression levels of *GAS41* (*upper*) and *p21* (*lower*) in 21 pairs of cancer versus adjacent non-cancerous tissues of human colorectal cancer patients. 16 out of 21 pairs (76.2%) showed higher expression of GAS41, and 11 of these 16 samples (68.8%) showed decreased p21. Shown were mean ± s.e.m. from 3 technical repeats of 21 paired samples.
(B) Relative mRNA expression levels of *GAS41* and *p21* in 21 non-cancer tissue samples. Mean of *GAS41* expression in 21 samples was set as 1.
(C) Scheme illustrating generation of HEK293T *GAS41* KO cells using CRISPR/CAS9 method. *Lower*, RT-qPCR analysis of *p21* expression in wild type and HEK293T *GAS41* KO cells, n=4.
(D) Western blot analysis and quantification of p21 expression in wt and HEK293T *GAS41* KO cells, n=3. *Right,* western blot analysis and quantification of p21 expression in HEK293T *GAS41* KO cells transfected with empty vector or Flag-GAS41 for 24h, n=3.
(E) Analysis of cell growth rate of wild type and HEK293T *GAS41* KO cells in a MTT assay. Shown were mean ± s.e.m. from 6 technical repeats. *Lower*, cell cycle analysis of wild type and HEK293T *GAS41* KO cells by fluorescence-activated cell sorter analysis. Relative distributions of cell cycle were analyzed using FlowJo software, n=3.

Figure S2, related to Figure 2

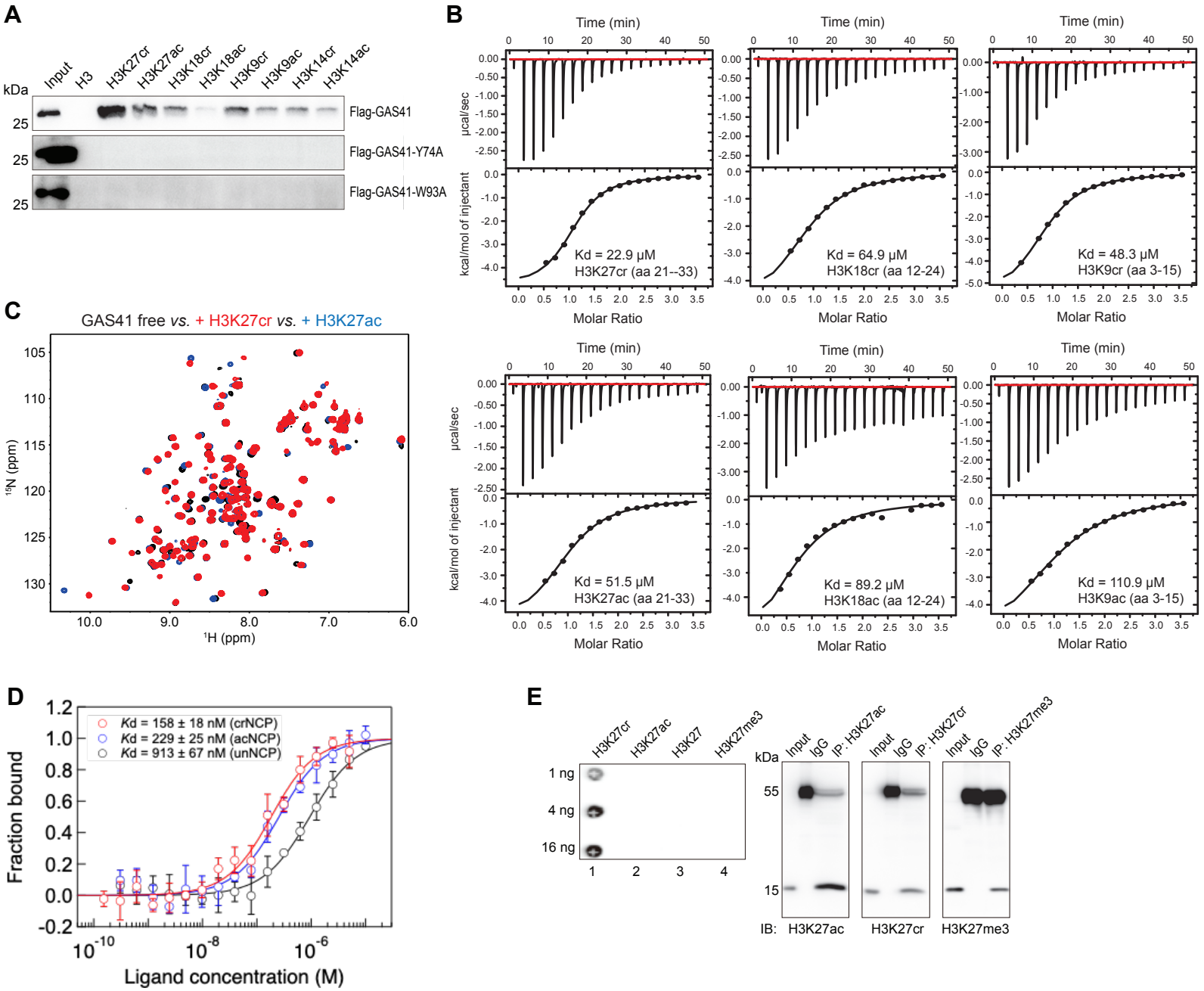

Figure S2. GAS41 YEATS domain prefers binding to H3K27cr over H3K27ac, related to Figure 2.

(A) Western blots showing ectopically expressed Flag-GAS41, Y74A or W93A mutant in HCT116 cells binding to a set of biotinylated peptides derived from histone H3 (residues 1-25, biotin-ARTK-QTARKSTGGKAPRKQLATKAA), H3K27cr/ac (residues 21-33, biotin-ATKAAR-Kcr/Kac-SAPAT-G), H3K18cr/ac (residues 12-24, biotin-GGKAPR-Kcr/Kac-QLATKA), H3K9cr/ac (residues 3-15, biotin-TKQTAR-Kcr/Kac-SSGGKA), and H3K14cr/ac (residues 1-25, biotin-ARTKQTARKSTGG-Kcr/Kac-APRKQLATKAA).

(B) ITC measurement of GAS41 YEATS domain binding to histone H3 peptides containing crotonyl-lysine (Kcr) or acetyl-lysine (Kac) at H3K27, H3K18, or H3K9 site. H3K27 (residues 21-33, ATKAAR-Kcr/Kac-SAPATG), H3K18 (residues 12-24, GGKAPR-Kcr/Kac-QLATKA), and H3K9 (residues 3-15, TKQTAR-Kcr/Kac-SSGGKA) peptides were used in the study.

(C) 2D ^{1}H-^{15}N-HSQC NMR spectra of the GAS41 YEATS domain depicting changes of backbone amide resonances upon addition of H3K27ac (blue) or H3K27cr (red) peptide.

(D) GAS41 YEATS domain binding affinity to nucleosome core particles (NCP) with or without histone H3K27cr or H3K27ac modification, as determined with microscale thermophoresis (MST) assay.

(E) Validation of the quality of the antibodies against H3K27cr, H3K27ac, and H3K27me3 by dot blotting (*left*) and antibody pull-down assay (*right*). Dot blotting analysis on crotonylated H3K27 (lane 1), acetylated H3K27 (lane 2), unmodified H3K27 (lane 3) and trimethylated H3K27 (lane 4) peptides of varying amounts as indicated using antibody against H3K27cr. Immunoprecipitation of endogenous H3K27ac, H3K27cr and H3K27me3 and immunoblotting with specific antibodies as indicated.

Figure S3, related to Figure 2

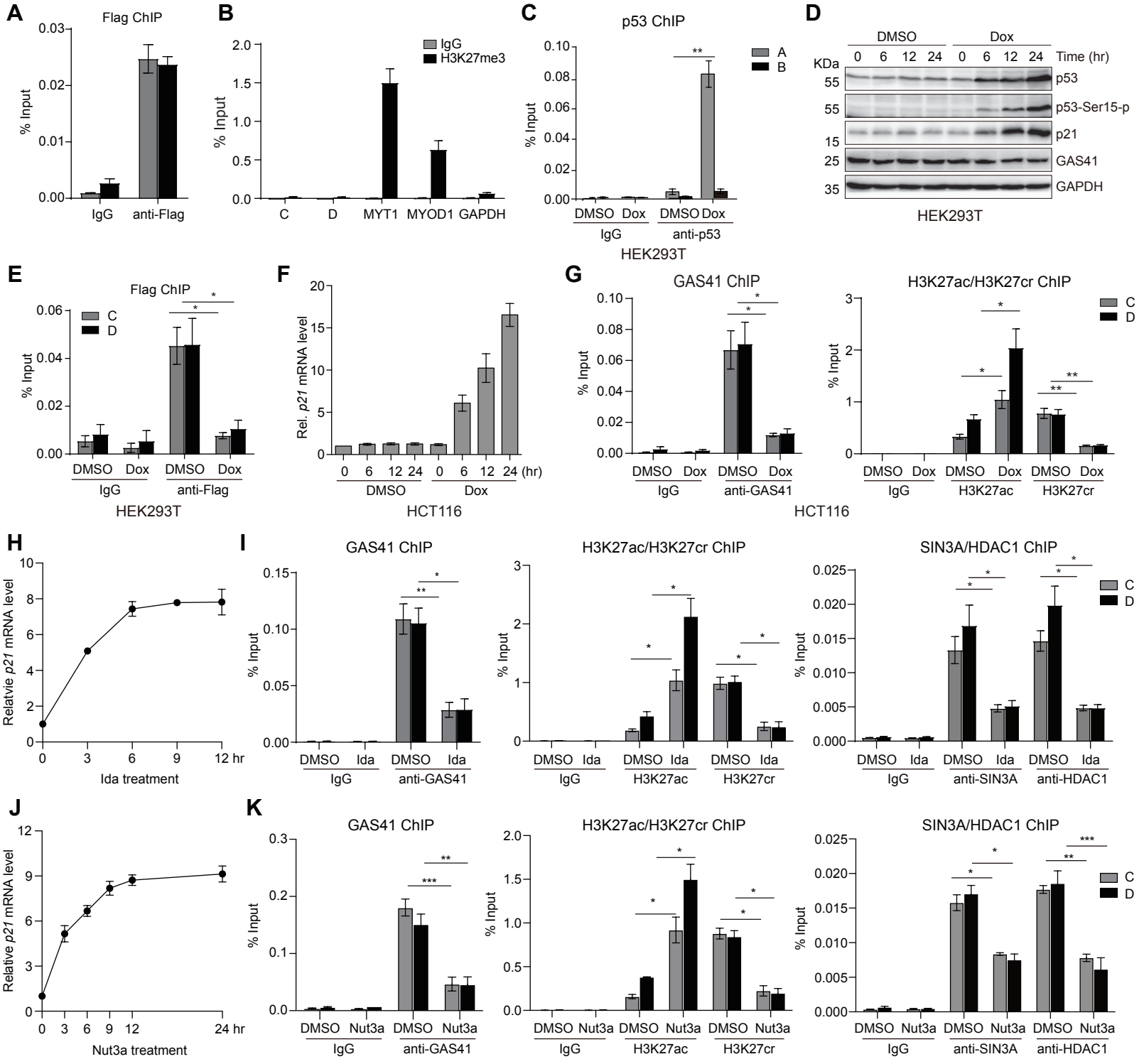

Figure S3. GAS41 dissociates from *p21* locus upon Dox treatment, related to Figure 2.

(A) ChIP-qPCR analyses of Flag-GAS41 enrichment at *p21* locus in Flag-GAS41-transfected HEK293T cells. n=3.

(B) The quality of H3K27me3 antibody was validated by ChIP of H3K27me3 at MYT1 and MYOD1 gene loci as positive controls and GAPDH as a negative control. Note that H3K27me3 presence at the C and D primer sites at the *p21* gene locus was negligible. n=3.

(C) ChIP-qPCR analysis of p53 enrichment at *p21* locus in HEK293T cells treated with Dox for 24 hours. n=3.

(D) Western blot analysis of p53, p53-Ser15-P, p21 and GAS41 expression levels in HEK293T cells upon Dox treatment for 0, 6, 12 and 24 hours, respectively. n=2.

(E) ChIP-qPCR showing changes of Flag-GAS41 level at *p21* locus in transfected HEK293T cells treated with Dox for 24 hours, n=3.

(F) mRNA transcript levels of *p21* in HCT116 cells treated with Dox for 0, 6, 12, and 24 hours, respectively. n=3.

(G) ChIP-qPCR analysis of GAS41, H3K27ac and H3K27cr enrichment at *p21* locus in HCT116 cells before and after 24-hour Dox treatment. n=3 for GAS41, 4 for H3K27cr and H3K27ac.

(H) mRNA transcript levels of *p21* in HEK293T cells treated with Idarubicin at 0.2μM for 0, 3, 6, 9, and 12 hours, respectively. n=3.

(I) ChIP-qPCR analysis of GAS41, H3K27ac and H3K27cr, and SIN3A/HDAC1 enrichment at *p21* locus in HEK293T cells after 6-hour Idarubicin treatment, n=3 for GAS41 and H3K27ac/H3K27cr ChIP, n=4 for SIN3A/HDAC1 ChIP.

(J) mRNA transcript levels of *p21* in HCT116 cells treated with Nutlin3a (5 μM), n=3.

(K) ChIP-qPCR analysis of GAS41, H3K27ac and H3K27cr, and SIN3A/HDAC1 enrichment at *p21* locus in HCT116 cells after 3-hour Nutlin3a treatment, n=3.

Figure S4, related to Figure 3

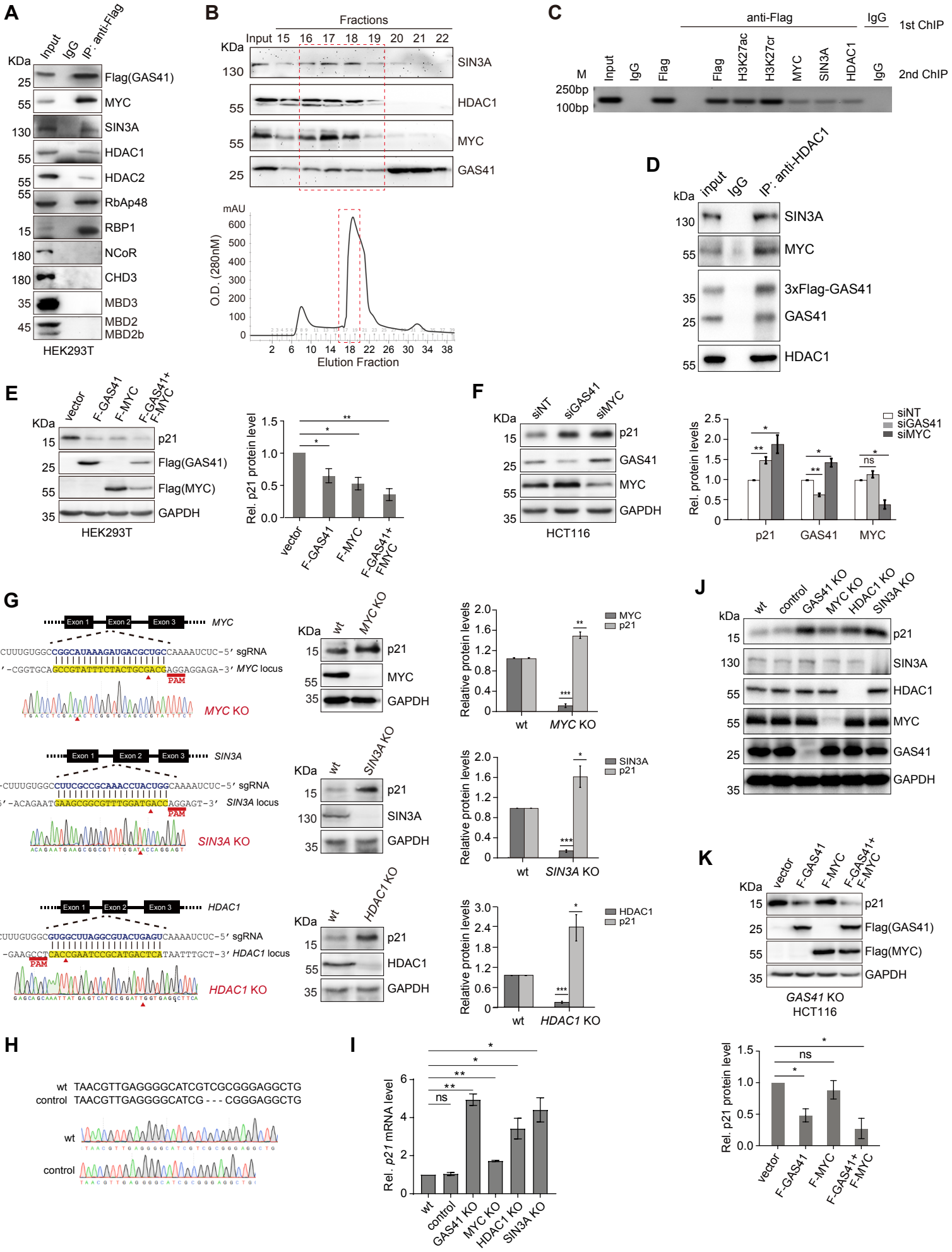

Figure S4. GAS41 works with MYC and SIN3A/HDAC1 co-repressors for *p21* repression, related to Figure 3.

(A) Co-IP of Flag-GAS41 and Western blots assessing GAS41 association with MYC, SIN3A, HDAC1/2, RbAp48, RBP1, NCoR, CHD3, and MBD2/3 in HEK293T cells.

(B) Western blots of SIN3A, MYC, HDAC1 and GAS41 in HCT116 cell lysates, from fractions 15-22 of size-exclusion chromatography using Superdex200 10/300 GL column (0.5 mL/fraction) (*lower*). n=6.

(C) Sequential ChIP showing co-localization of Flag-GAS41, H3K27ac, H3K27cr, MYC, SIN3A, and HDAC1 in HCT116 cells. n=3.

(D) Western blot analysis of HDAC1 Co-IP showing MYC/SIN3A-HDAC1 association with endogenous GAS41 and 3xFlag-GAS41 in HCT116 cells. n=3.

(E) Western blots and quantification of p21 expression in HEK293T wild type cells transfected with Flag-GAS41 and Flag-MYC, n=4.

(F) Western blots and quantification of p21, GAS41, MYC expression in HCT116 cells transfected with *GAS41* and *MYC* siRNAs, n= 4.

(G) Schemes depicting guide RNA design targeting *MYC, HDAC1* or *SIN3A* start codon to generate gene KO in HEK293T cells with CRISPR/Cas9 (*left*). Clones selected carried 4-base deletion for *MYC* KO, one-base deletion for *SIN3A* and *HDAC1* KO at indicated positions, resulting in premature stop codon and protein disruption. Western blots (*middle*) and quantification (*right*) of p21 expression in wild type and KO cells, n=4-5.

(H) Sanger sequencing results showing the three-base deletion in the non-coding 5' UTR (upstream of ATG) of MYC gene locus in the two alleles of control cells.

(I) RT-qPCR analysis of *p21* mRNA levels in wild type, control, *GAS41* KO, *MYC* KO, *HDAC1* KO and *SIN3A* KO cells. Statistical significance was determined between wild type and the corresponding KO groups. n=3.

(J) Western blots showing p21, SIN3A, MYC, HDAC1 and GAS41 expression levels in HEK293T wt, control, *GAS41* KO, *MYC* KO, *HDAC1* KO and *SIN3A* KO cells. n=3.

(K) Western blots and qualification of *p21* expression in HCT116 *GAS41* KO cells transfected with Flag-GAS41 and Flag-MYC. n=3

Figure S5, related to Figure 3

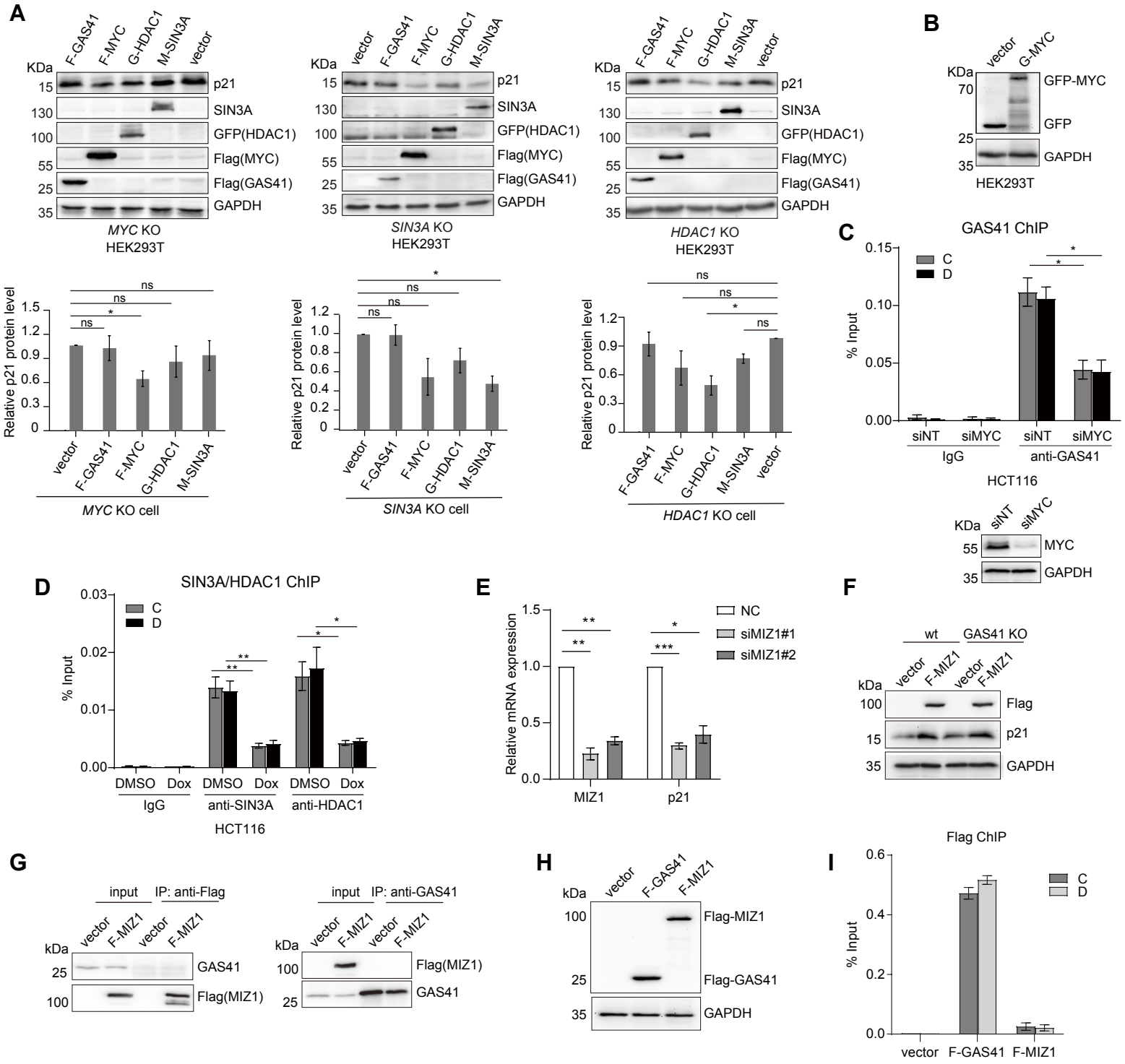

Figure S5. GAS41 works with MYC and SIN3A/HDAC1 co-repressors for *p21* repression, related to Figure 3.

(A) Western blot analysis and quantification of p21 expression in HEK293T *MYC*, *SIN3A*, or *HDAC1* KO cells transfected with F-GAS41, F-MYC, G-HDAC1 and M-SIN3A. n=3 for *SIN3A* and *HDAC1* KO cells, and n=4 for *MYC* KO cells.

(B) Western blot analysis of GFP and GFP-MYC expression in HEK293T cells transiently transfected with GFP and GFP-MYC, related to **Figure 3E**.

(C) Western blot analysis of MYC expression, and ChIP-qPCR analysis of GAS41 enrichment at *p21* locus in HCT116 cells transfected with NT and MYC siRNAs. n=4

(D) ChIP-qPCR analysis of SIN3A and HDAC1 enrichment at *p21* locus in HCT116 cells before and after 24-hour Dox treatment. n=4.

(E) p21 mRNA levels in HCT116 cells transfected with MIZ1 siRNAs, assessed by RT-qPCR analysis. n=3.

(F) Effects of Flag-MIZ1 on p21 expression in GAS41 wild type and KO cells transfected with Flag-MIZ1.

(G) Assessing Flag-MIZ1 binding to GAS41 by reciprocal Co-IP assays.

(H) Western blots showing protein levels of Flag-GAS41 and Flag-MIZ1 in HCT116 cells.

(I) Chromatin occupancy of Flag-GAS41 and Flag-MIZ1 at the p21 locus in HCT116 cells transfected with Flag-MIZ1 and Flag-GAS41 by ChIP-qPCR analysis. n=3.

Figure S6, related to Figure 4

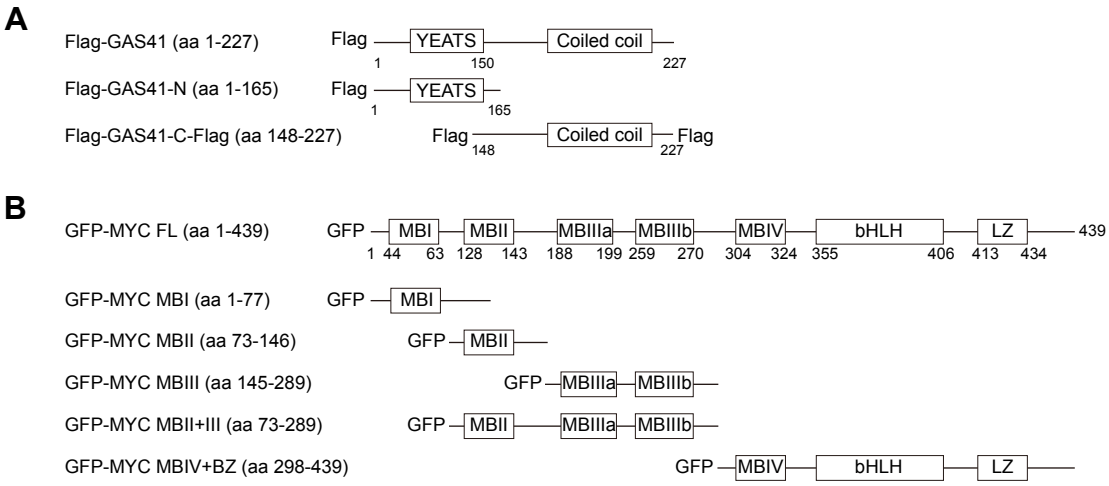

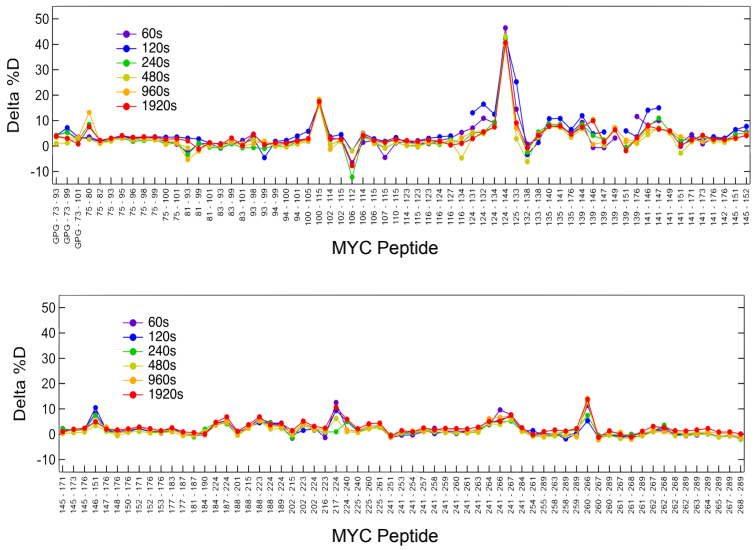

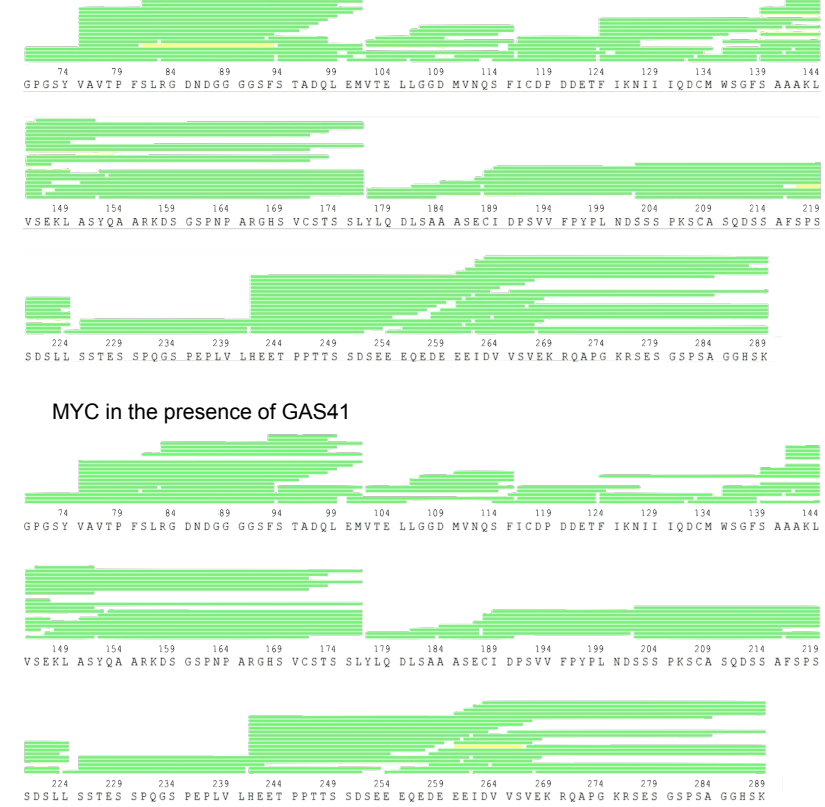

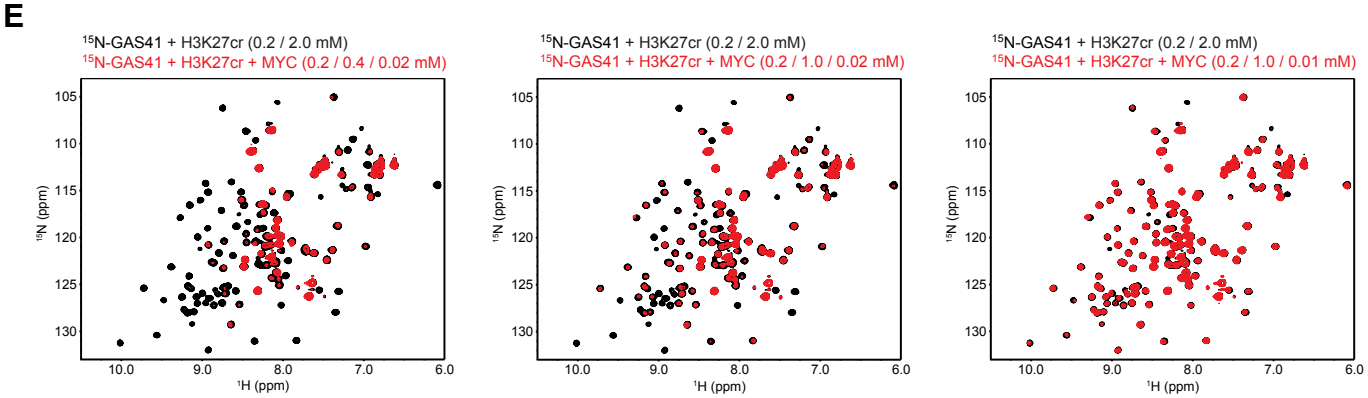

Figure S6. GAS41 interacts with H3K27cr and MYC, related to Figure 4.

(A) Schematic illustration of Flag-GAS41 and its segment constructs.

(B) Schematic illustration of GFP-MYC and its segment constructs.

(C) Differences of the deuteration level of MYC (residues 73-289) with or without GAS41 YEATS domain (residues 11-150), as determined in the hydrogen/deuterium exchange followed by mass spectrometry (HDX-MS) analysis.

(D) Identified fragmented peptides of MYC in the absence (upper) and presence (lower) of GAS41 YEATS domain in the HDX-MS experiment in **C**. Peptides were indicated as green or yellow bars, which stand for high and medium confidence, respectively, and aligned along the protein sequence.

(E) Analysis of MYC (residues 1-262) *vs.* H3K27cr peptide binding to the GAS41 YEATS domain, as assessed by 2D ^{1}H-^{15}N-HSQC NMR spectra of GAS41 YEATS domain/MYC complex in the varying amounts of H3K27cr peptide.

Figure S7, related to Figure 5

A

```
                 11        20                  40                  60                  80
                 |         |    β1       *     |     *     β2        |α1    β3   * **    β4|    *   β5  *
GAS41(YEATS4)    DSGGRVKGVTIVKPIVYGNVARYFGKKREEDG---HTHQWTVYVKPYRNE-DMSAYVKKIQFKLHESYG-NPLRVVTKPPYEITETGWGE   1-95
AF9(MLLT3)           MASSCAVQVKLELGHRAQVR-KKPTVEG---FTHDWMVFVRGPEHS-NIQHFVEKVVFHLHESFP-RPKRVCKDPPYKVEESGYAG   1-80
ENL(MLLT1)           MDNQCTVQVRLELGHRAQLR-KKPTTEG---FTHDWMVFVRGPEQC-DIQHFVEKVVFWLHDSFP-KPRRVCKEPPYKVEESGYAG   1-80
YEATS2               ETSRLFVKKTIVVGNVSKYIPPDKREEND-QSTHKWMVYVRGSRREPSINHFVKKVWFFLHPSYKPNDLVEVREPPFHLTRRGWGE   200-284
Yaf9                 RIKTLSVSRPIIYGNTAKKMGSVKPPNAPAEHTHLWTIFVRGPQNE-DISYFIKKVVFKLHDTYP-NPVRSIEAPPFELTETGWGE   8-93
Taf14                MVATVKRTIRIKTQQHILPEVPP-VENFPVRQWSIEIVLLDDEGKE-IPATIFDKVIYHLHPTFA-NPNRTFTDPPFRIEEQGWGG   1-83
Sas5                 MDHSIEVTFRVKTQQVIIPEQNIRGNELPLRRWQMELLMLDATGKE-VEPTILSKCIYHLHSSFK-QPKRRLNSLPFFIKETGWGE   1-84

                      100               120                 140                 160
                      * β6|      β7     |*   α2  *          β8*|                 |
GAS41(YEATS4)         FEIIIKIFFIDPN-ERPVTLYHLLKLFQSDTNAML--------------GKKTVVSEFYDEMIFQDPTAMMQQLLTTSR-          96-159
AF9(MLLT3)            FILPIEVYFKNKEEPRKVRFDYDLFLHLEG-------------------HPPVNHLRCEKLTFNNPTTEDFRRKLLKA---          81-138
ENL(MLLT1)            FIMPIEVHFKNKEEPRKVCFTYDLFLNLEG-------------------NPPVNHLRCEKLTFNNPTTEFRYKLLRA---          81-138
YEATS2                FPVRVQVHFKDS-QNKRIDIIHNLKLDRTYTGLQ---------------TLGAETVVDVELHRHSLGEDCIYPQSSE---          285-345
Yaf9                  FDINIKVYFVEEANEKVLNFYHRLRLHPYANPVPNSDNGNEQNTTDHNSKDAEVSSVYFDEIVFNEPNEEFFKILMSR--          94-171
Taf14                 FPLDISVFLLEKAG--ERKIPHDLNFLQ-----------------------ESYEVEHVIQIPLNKPLLTEELAKSGST          84-137
Sas5                  FNLKIECFFIGNAGKFSIEHDLTFEDDAYA----------------------VDYTVDVPHEFSHLNSELSKYFDLP---          85-139
```

B

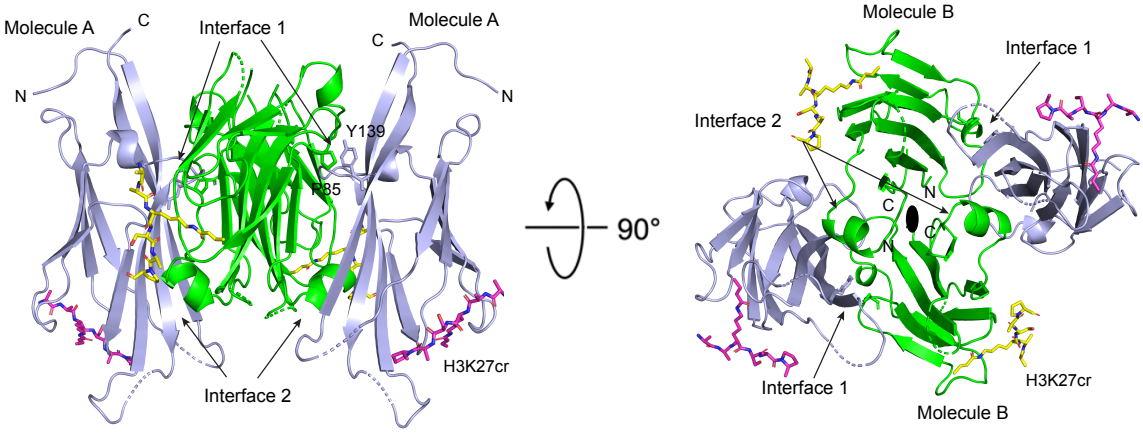

C

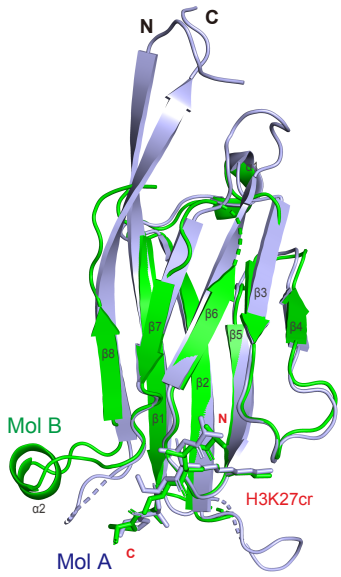

Figure S7. Structural basis of GAS41 YEATS domain binding to H3K27cr and MYC, related to Figure 5.

(A) Structure-based protein sequence alignment of the YEATS domains in human and yeast proteins. The key amino acid residues of GAS41 engaged in crotonylated-Lys27 of the H3K27cr peptide binding are highlighted by black asterisk, Pro30 of the H3K27cr peptide by red asterisk, Tyr135 and Pro85 at the dimer interface by blue asterisk.

(B) Crystal structure of GAS41 YEATS domain as a tetramer, consisting of a dimer of dimer, color-coded in light blue and green, depicted as side (*left*) and top (*right*) views. Histone H3K27cr peptide bound in Molecule A and Molecule B are highlighted in magenta and yellow, respectively. A short α-helix (residues 123-128) at the Interface 2 is indicated, whereas side chains of P85 and Y139 at the Inter- face 1 are shown.

(C) Superimposition of two protomers (Mol A in light blue and Mol B in green) of GAS41 YEATS domain/H3K27cr peptide complex in an asymmetric unit.

Figure S8, related to Figure 5

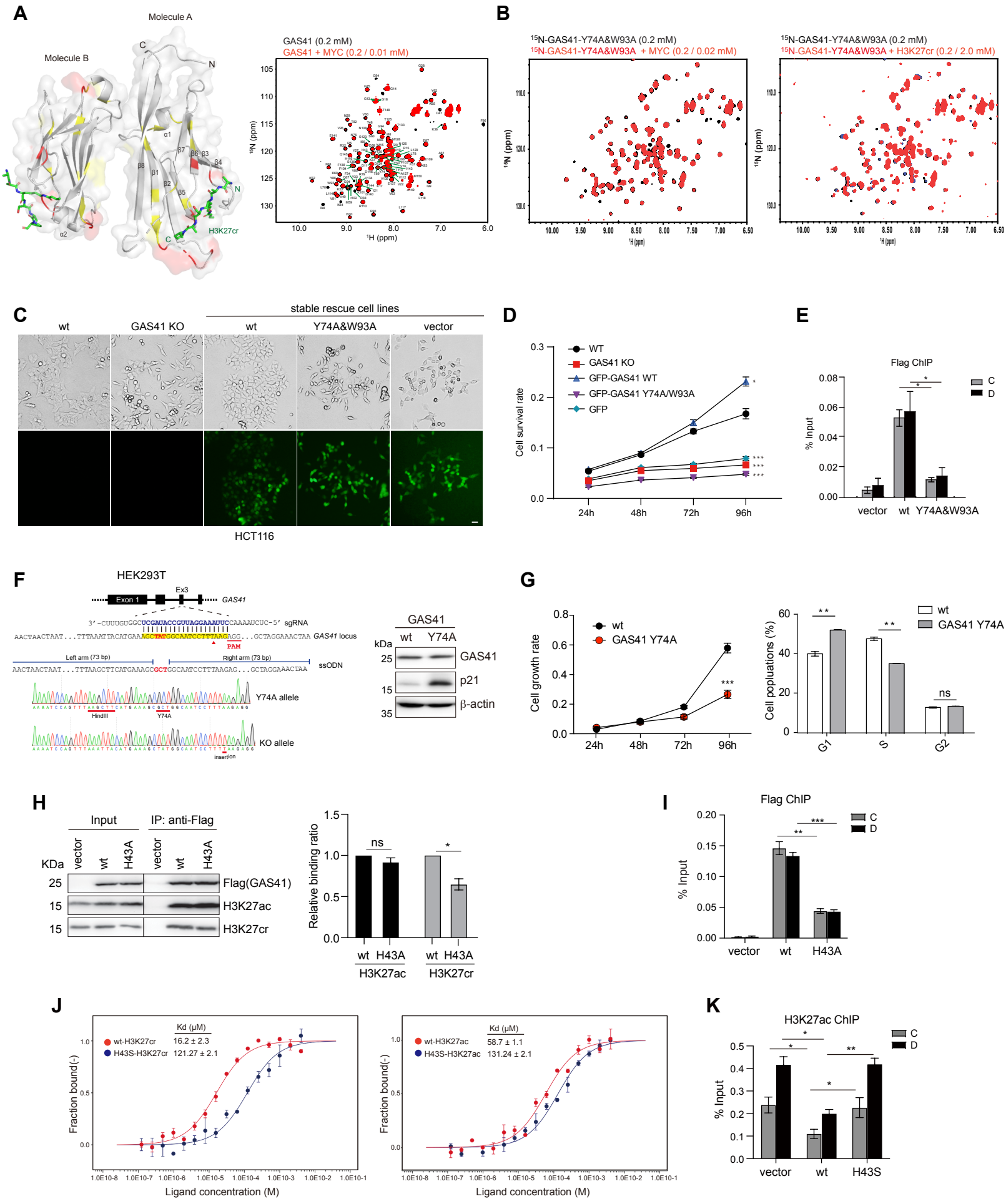

Figure S8. H3K27cr binding deficient GAS41 induces *p21* de-repression, related to Figure 5.

(A) Mapping of MYC binding site in the GAS41 YEATS domain through assessing protein residues whose backbone amide signals exhibited line-broadening-induced disappearance (colored in red), or severe intensity reduction (yellow) in 2D ^{1}H-^{15}N-HSQC NMR spectra upon addition of purified N-terminal MYC protein (residues 1-262), depicted in *right* panel.

(B) The binding of mutant GAS41 YEATS domain Y74A&W93A to MYC (*left* panel, residues 1-262) or H3K27cr peptide (*right* panel), assessed by 2D ^{1}H-^{15}N-HSQC NMR spectra.

(C) Representative images (upper, phase-contrast; lower, GFP-tagged protein) of HCT116 GAS41 KO cells stably expressing GFP-Flag-GAS41 wt, mutant GFP GAS41 Y74A&W93A and vector. Scale bar 10 μm.

(D) Analysis of cell growth rate of HCT116 wt, *GAS41* KO and *GAS41* KO cell stably expressing GFP-Flag-GAS41 wt, mutants and vector by MTT assay. Shown was mean ± s.e.m. from 5 technical repeats. Statistical analysis was calculated using respective values to wt.

(E) ChIP-qPCR analysis of Flag-GAS41 wild type and Y74A&W93A mutant occupancy at the *p21* locus in *GAS41* KO HCT116 cells stably expressing GFP-Flag-GAS41 wild type, Y74A&W93A mutant, or empty vector. n=3.

(F) Schematic representation of generating HEK293T cells containing mutant GAS41 Y74A with CRISPR-Cas9 method (*left*) and west- ern blot analysis of p21 expression in wt HEK293T and mutant HEK293T containing GAS41 Y74A cells (*right*).

(G) Analysis of cell growth rate of HEK293T cells and HEK293T with Y74A mutation cells by MTT assay. Shown are mean ± s.e.m. from 6 technical repeats. *Right*, cell cycle analysis of wild type HEK293T cells and HEK293T cells containing mutant GAS41 Y74A by fluorescence-activated cell sorter analysis. Relative distributions of cell cycle were analyzed using FlowJo software, n=3.

(H) CoIP analysis and quantification of H43A mutant on GAS41 binding to H3K27ac and H3K27cr. The lysate of HCT116 cells transfect- ed with Flag-GAS41 wild type and H43A was subjected to Flag IP and followed by IB with antibodies against Flag, H3K27ac and H3K27cr, respectively, n=3.

(I) ChIP-qPCR analysis showing Flag-GAS41 occupancy at *p21* locus in HCT116 cells transiently expressing Flag-GAS41 wt and H43A, n=3.

(J) Binding affinity of mGFP-GAS41 wild type or H43S mutant binding to H3K27ac or H3K27cr peptide as determined using microscale thermophoresis. Data was the average of three replicates and K_d was obtained by fitting Hill model.

(K) ChIP-qPCR analysis showing H3K27ac level at *p21* locus in HCT116 cells transiently expressing Flag-GAS41 wild type and H43S, n=3.

Figure S9, related to Figure 6

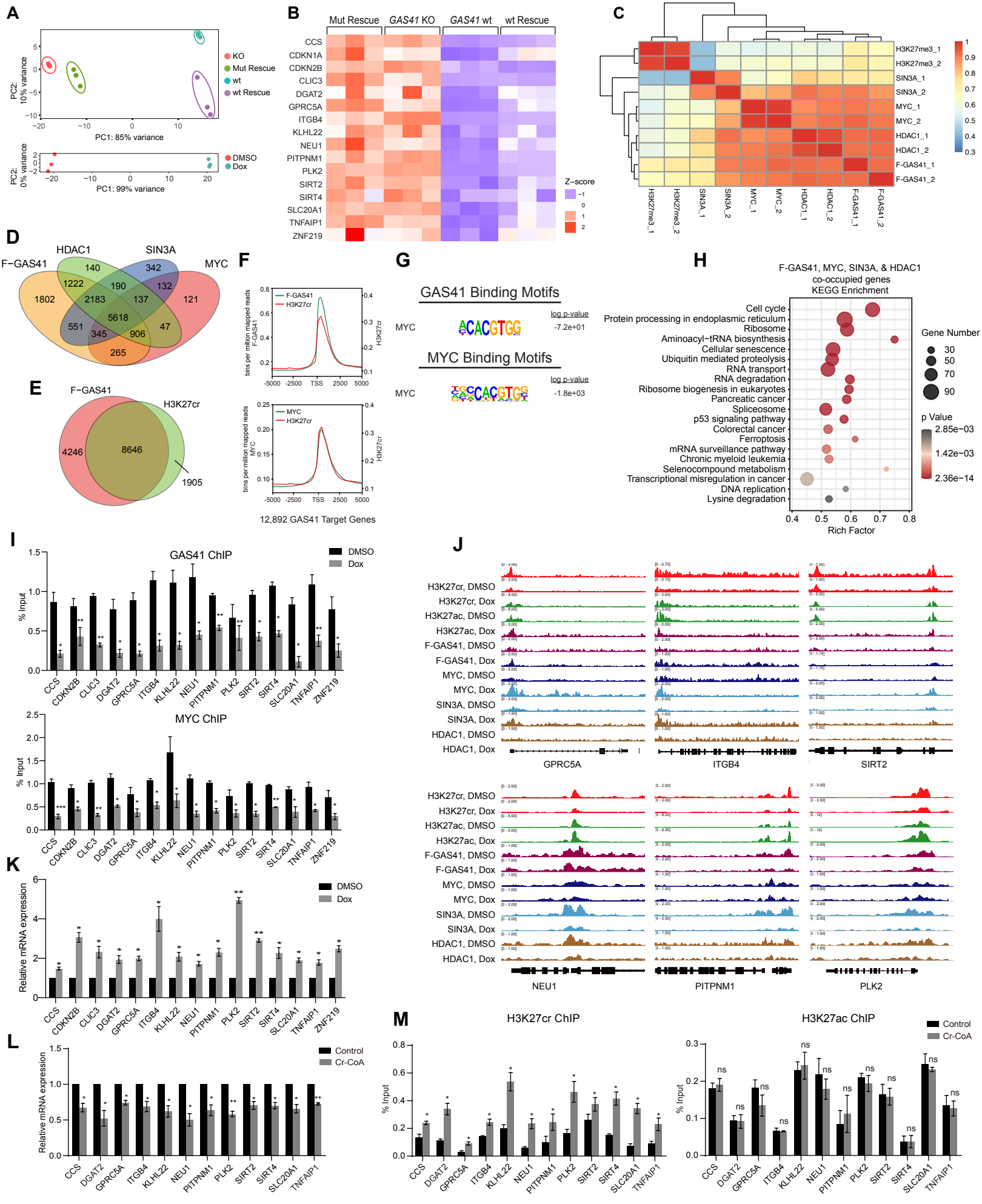

Figure S9. H3K27cr marks for gene repression by the GAS41/MYC/SIN3A-HDAC1 co-repressor complex, related to Figure 6.

(A) PCA plots of RNA-seq data from **Figure 6A** (upper) and **Figure 6H** (lower).

(B) Heatmap of selected genes differentially expressed in HCT116 GAS41 wild type and KO cells, as well as *GAS41* KO cells that stably expressed GAS41 wild type or mutant Y74A/W93A rescue, as shown in **Figure 6A**.

(C) Heatmap showing correlation of genomic occupancy of F-GAS41, MYC, SIN3A and HDAC1 as indicated by their ChIP-seq peaks in HCT116 cells. H3K27me3 ChIP-seq peaks used as a negative control.

(D) Venn diagram showing overlap of F-GAS41, MYC, SIN3A and HDAC1 occupied genes identified from our ChIP-seq data in HCT116 cells.

(E) Venn diagram showing overlap of F-GAS41 and H3K27cr occupied genes identified from our ChIP-seq data in HCT116 cells.

(F) ChIP-seq peaks of Flag-GAS41, or MYC *vs.* H3K27cr, centered at the TSS (±5kb) of 12,892 GAS41 target genes in HCT116 cells. Reads were normalized to bins per million mapped reads.

(G) DNA binding motifs identified for GAS41 and MYC from their ChIP-seq data in HCT116 cells using the Homer program.

(H) KEGG enrichment analysis of genes co-occupied by F-GAS41, MYC, SIN3A and HDAC1 identified from our ChIP-seq data in HCT116 cells, as in **Figure S9D**. The top 20 categories are shown. Bioinformatic analysis was performed using the OmicStudio tools.

(I) ChIP-qPCR analysis of GAS41 and MYC occupancy at the selected GAS41 target gene loci, as in **Figure 6H,** in HCT116 cells before and after Dox treatment. n=3. Values are normalized to DMSO control.

(J) H3K27cr, H3K27ac, F-GAS41, MYC, SIN3A and HDAC1 ChIP-seq peaks as illustrated at selected genes *GPRC5A, ITGB4, NEU1, PITPNM1, PLK2* and *SIRT2* loci in HCT116 cells treated with DMSO and Dox.

(K) qPCR analysis of mRNA levels of GAS41 target genes, as in **Figure 6H,** in HCT116 cells before and after Dox treatment. n=3.

(L) qPCR analysis of mRNA levels of GAS41 target genes in HEK293T cells with or without Cr-CoA (50 μM) treatment for 24 hours. n=3.

(M) ChIP-qPCR analysis of H3K27cr and H3K27ac levels at the selected GAS41 target gene loci in HEK293T cells before and after Cr-CoA (50 μM) treatment for 24 hours. n=3.

Figure S10, related to Figure 6

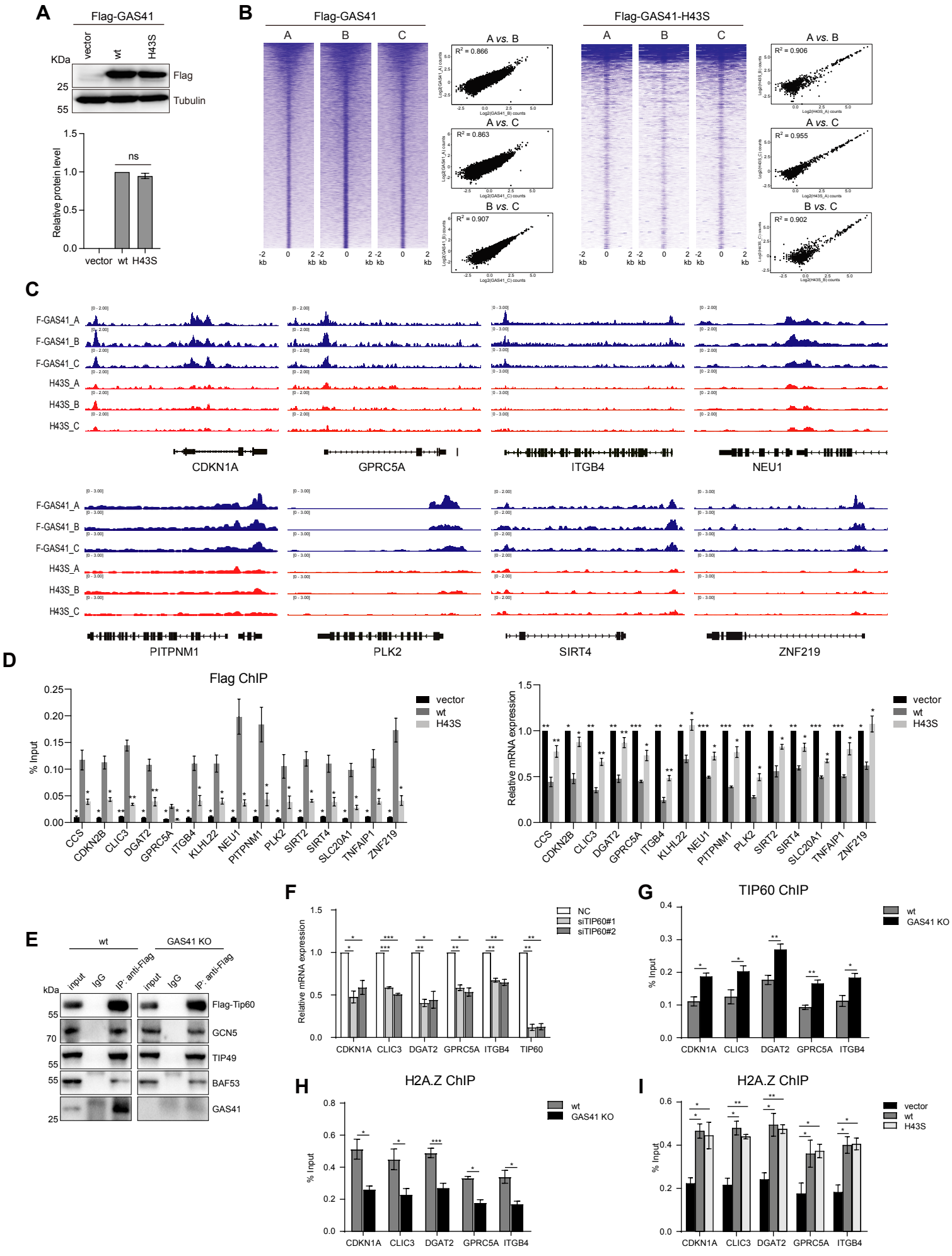

Figure S10. H3K27cr binding is required for GAS41 function in gene transcriptional repression, related to Figure 6.

(A) Western blot analysis showing HCT116 GAS41 KO cells stably expressing Flag-GAS41 wild type or H43S mutant. *Lower panel,* quantification and statistical analysis of the expression levels of Flag-GAS41 wild type and H43S mutant. n=3.

(B) Statistical analysis of ChIP-seq datasets of Flag-GAS41 wild type and H43S mutant, generated in HCT116 GAS41 KO cells, stably expressing Flag-GAS41 or H43S mutant.

(C) ChIP-seq peaks of Flag-GAS41 wild type and H43S mutant triplicates as illustrated at selected genes CDKN1A (p21) GPRC5A, ITGB4, NEU1, PITPNM1, PLK2, SIRT4, ZNF219.

(D) ChIP-qPCR analysis showing Flag-GAS41 wild type or H43S mutant at the selected GAS41 target gene loci. *Right panel,* qPCR analysis showing mRNA transcript levels of the selected GAS41 target genes. n=3, statistical analysis was calculated by comparing vector to wild type and H43S to wild type, respectively.

(E) Western blot analysis of Flag-TIP60 interactions with TIP49, GCN5, BAF53 and GAS41 in Co-IP assay.

(F) RT-qPCR analysis of GAS41 targets expression in HCT116 cells transfected with TIP60 siRNAs. n=3.

(G, H) ChIP-qPCR analyses showing changes of TIP60 and H2A.Z in HCT116 wild type and GAS41 KO cells. n=3.

(I) ChIP-qPCR analyses showing changes of H2A.Z in HCT116 GAS41 KO cells stably expressing Flag-vector, Flag-GAS41 wild type or H43S. n=3.

Table S1. Hydrogen/deuterium exchange–mass spectrometry (HDX-MS) analysis, related to Figure 4

Data Set	MYC	MYC / GAS41
HDX time course (sec)	60, 120, 240, 480, 960, 1920	60, 120, 240, 480, 960, 1920
Number of peptides	146	132
Sequence coverage (%)	100.00	100.00
Average peptide length / Redundancy	18.01 / 11.95	18.07 / 10.84

Table S2. Crystallography data and refinement statistics o the GAS41/H3K27cr complex structure, related to Figure 5

Parameters	GAS41/H3K27cr
Data collection	
Space group	$P4_12_12$
Cell dimensions	
a, b, c (Å)	91.98, 91.98, 83.41
α, β, γ (°)	90, 90, 90
Resolution (Å)	61.79-2.30 (2.38-2.30)*
Measured reflections	195334 (25365)
Unique reflections	16481 (2342)
R_{merge}	13.3 (43.0)
I/σ	11.5 (5.0)
$CC_{1/2}$	0.995 (0.920)
Completeness (%)	100.0 (99.9)
Redundancy	11.9 (10.8)
Refinement	
Resolution (Å)	61.79-2.30
No. reflections (test set)	16429 (1600)
R_{work}/R_{free} (%)	25.6/29.1
No. of atoms	
Protein	1719
Peptide	83
Water	57
B-factors (Å)	
Protein	48.6
Peptide	55.3
Water	46.3
rmsd	
Bond length (Å)	0.008
Bond angles (°)	1.20
Ramachandran plot, % residues	
Favored	86.6
Additional allowed	13.4
Generously allows	0
Disallowed	0

*Values in parentheses are for the highest resolution shell.

Table S4. Oligonucleotide Sequences Used for siRNAs, CRISPR/Cas9, qPCR, and ChIP-qPCR, Related to the STAR Methods

A. Oligonucleotide sequences for siRNAs		
Gene	**Sense**	**Anti-sense**
GAS41	AUAGUAACACCCUUUACUCUC	GAGUAAAGGGUGUUACUAUCG
c-Myc	GGAAGAAAUCGAUGUUGUUTT	AACAACAUCGAUUUCUUCCTT
B. Oligonucleotide sequences for generating GAS41 knockout and GAS41 Y74A cell lines		
	Top oligo	**Bottom oligo**
GAS41 KO	CACCGTCAAGAGAATGGCCGAATTT	AAACAAATTCGGCCATTCTCTTGAC
c-Myc KO	CACCGGCCGTATTTCTACTGCGACG	AAACCGTCGCAGTAGAAATACGGCC
HDAC1 KO	CACCGTGAGTCATGCGGATTCGGTG	AAACCACCGAATCCGCATGACTCAC
SIN3a KO	CACCGGAAGCGGCGTTTGGATGACC	AAACGGTCATCCAAACGCCGCTTCC
GAS41 Y74A	CACCGAGCTATGGCAATCCTTTAAG	AAACCTTAAAGGATTGCCATAGCTC
Y74A ssODNS	AACTAACTAATTCCTTATATTTTAGGATATGTCAGCATATGTGAAGAAAATCCAGTTTAAGCT TCATGAAAGCGCTGGCAATCCTTTAAGAGGTACAATATAGTCTTTTGATTCACAATATCCAA AGTTAAAAATGGCTAGGAAACTAA	
C. Sequences for RT-qPCR primers		
Gene	**Sense**	**Antisense**
GAS41	ACTCCGGCGGGAGAGTAAA	TGAGTGTGCCCATCTTCTTCTC
p21	GGCAGACCAGCATGACAGAT	GATGTAGAGCGGGCCTTTGA
c-Myc	AGCATACATCCTGTCCGTCC	GCACAAGAGTTCCGTAGCTG
GAPDH	GTGAAGGTCGGAGTCAACGG	CCTGGAAGATGGTGATGGGA
CDKN2B	GGTGAACCCACAACTTAGGC	TTAGCATCTGTCGTCGCTTG
PLK2[79-81]	CTACGCCGCAAAAATTATTCCTC	TCTTTGTCCTCGAAGTAGTGGT
ITGB4[79-81]	GCTTCACACCTATTTCCCTGTC	GACCCAGTCCTCGTCTTCTG
SLC20A1	ATGTCTTGGTTCGTGTCCCC	CAGCAACGGTGCTCCAGTAT
ZFP36L1	CTTCGCGACACACCAGATCC	TTTCTGTCCAGCAGGCAACC
SIRT4[79-81]	AGCCTCCATTGGGTTATTTGTG	TCTGGTATCCCCGATTCGGT
FOS[79-81]	CCGGGGATAGCCTCTCTTACT	CCAGGTCCGTGCAGAAGTC
JUN	TGAGTGACCGCGACTTTTCA	TTTCTCTAAGAGCGCACGCA
TLCD1[79-81]	TGTTAGTGGAGATTGAGACGGC	GTGGATGAAATACCCCGCAG
GPRC5A	GCTGCTCACAAAGCAACGAA	ATAGAGCGTGTCCCCTGTCT
D. Sequences for ChIP-qPCR primers		
Sites	**Sense**	**Antisense**
-2283 (A)[82]	AGCAGGCTGTGGCTCTGATT	CAAAATAGCCACCAGCCTCTTCT
-1391 (B)[82]	CTGTCCTCCCCGAGGTCA	ACATCTCAGGCTGCTCAGAGTCT
CDKN2B	TTTTGTCTTATGTGTGCCAGGTTG	GAATCATGTTTTGCGTGTGCTTTTTAATTC
PLK2	TGCCATCCTCAATTCCGTCT	TTTGCGGCGTAGACTTTGTT
ITGB4	CACACCCTGAGGACAAGGAC	AGACTCCAAGCCTTCACTGC
SLC20A1	ATGGAATTCTGCTCCGTGCT	TGCGTATGGGCATCTGTTGT
ZFP36L1	TGAGAATGCGCTCTCTTCGG	GCTGCGGAGTGGCTAAGATT
SIRT4	ACGAAACAGCTTCCAAGATCTGA	TCATATTGTATCCCACTTTTTCCCA

FOS	TGAAGGGATAACGGGAACGC	ATCCTGCCACGGACATTTCA
JUN	CAGCCAGGTCGGCAGTATAG	TCTGGACACTCCCGAAACAC
TLCD1	TGGTATAGGCCTGGTGTCAGT	AGAAGTAGCACACAGGTCGG
GPRC5A	TTCTCTTGATGTGTGGGCGG	AAGTCGGTAGTGGAAGGTGC